Available online at www.sciencedirect.com
ScienceDirect
Proceedings of the Combustion Institute 000 (2022) 1–10
Proceedings of the Combustion Institute
www.elsevier.com/locate/proci

Stochastic low-order modelling of hydrogen autoignition in a turbulent non-premixed flow

Salvatore Iavarone [a,b,*], Savvas Gkantonas [a], Epaminondas Mastorakos [a]

[a] University of Cambridge, Department of Engineering, Cambridge, UK
[b] Université Libre de Bruxelles, École Polytechnique de Bruxelles, Aero-Thermo-Mechanics Laboratory, Brussels, Belgium

Received 5 January 2022; accepted 12 July 2022
Available online xxx

Abstract

Autoignition risk in initially non-premixed flowing systems, such as premixing ducts, must be assessed to help the development of low-NO_x systems and hydrogen combustors. Such situations may involve randomly fluctuating inlet conditions that are challenging to model in conventional mixture-fraction-based approaches. A Computational Fluid Dynamics (CFD)-based surrogate modelling strategy is presented here for fast and accurate predictions of the stochastic autoignition behaviour of a hydrogen flow in a hot air turbulent co-flow. The variability of three input parameters, i.e., inlet fuel and air temperatures and average wall temperature, is first sampled via a space-filling design. For each sampled set of conditions, the CFD modelling of the flame is performed via the Incompletely Stirred Reactor Network (ISRN) approach, which solves the reacting flow governing equations in post-processing on top of a Large Eddy Simulation (LES) of the inert hydrogen plume. An accurate surrogate model, namely a Gaussian Process, is then trained on the ISRN simulations of the burner, and the final quantification of the variability of autoignition locations is achieved by querying the surrogate model via Monte Carlo sampling of the random input quantities. The results are in agreement with the observed statistics of the autoignition locations. The methodology adopted in this work can be used effectively to quantify the impact of fluctuations and assist the design of practical combustion systems.

Keywords: Autoignition; Non-premixed flames; Low-order modelling; Stochastic modelling; Hydrogen

1. Introduction

Modelling slow reactions leading to autoignition in turbulent non-premixed flows is important for a range of applications. Practical devices may include fluctuations in the values of inlet parameters, such as temperature, velocity, and composition, whose impact must be understood and predicted with affordable tools. Such fluctuations may cause autoignition in locations or timings away from the design point and create a risk for combustion concepts such as low-NO_x gas turbines or future hydrogen combustion systems. This work presents a strategy to capture the stochasticity of

* Corresponding author.
E-mail addresses: si339@cam.ac.uk, salvatore.iavarone@ulb.be (S. Iavarone).

https://doi.org/10.1016/j.proci.2022.07.129

the autoignition process due to parameter fluctuations in a turbulent non-premixed configuration, using accepted deterministic modelling approaches based on the mixture fraction concept.

Computational Fluid Dynamics (CFD) simulations of turbulent autoignition must include both turbulent mixing and detailed chemistry [1]. A considerable number of simulations at different operating conditions may be required for practical systems design. Moreover, autoignition may happen randomly if temperature, velocity, and species composition vary around the design condition due to even small, naturally occurring fluctuations. Hence, a strategy to capture the stochasticity of the autoignition process due to parameter fluctuations is necessary. A solution can be provided by *forward* Uncertainty Quantification (UQ) approaches, which determine the uncertainty in the prediction of selected quantities due to the known variability of input and model parameters, usually described by probability density functions (PDFs). In combustion studies, forward propagation of uncertainties provided prediction intervals on laminar flame speeds [2,3], ignition delay times [4,5], and NO_x emissions [6–8]. Monte Carlo methods are the most direct forward UQ approach, but they require a large number of realisations. When the realisations are obtained by costly CFD simulations, Monte Carlo methods become computationally unfeasible. Several studies focused on solving this issue by either reducing the number of Monte Carlo samples needed to compute the output PDFs accurately [9,10] or using surrogate models (also called meta-models) [11,12]. Surrogate models are low-order functions constructed (trained) upon a reduced number of CFD simulations and replace the latter in mapping input/output quantities. However, depending on the computational cost of the simulations needed and the dimensionality of the uncertain input space, the training of accurate surrogate models may still be practically unfeasible. Thus, there is a need to employ computationally inexpensive methods that simplify calculations with detailed turbulence and chemistry models and capture system responses to perturbations without significant loss of accuracy.

Markides and Mastorakos [13–15] performed experiments of autoignition of hydrogen, heptane and acetylene plumes, diluted with nitrogen, issued into a turbulent co-flow of preheated air. Different autoignition regimes, i.e., "no ignition", "random spots", flashback, and lifted flame, were observed depending on the co-flow temperature and the ratio between co-flow and fuel velocities. Moreover, PDFs of autoignition spot locations were obtained from OH^* chemiluminescence and measurements of the inlet temperature fluctuations were performed, rendering this experiment ideal for validating the proposed approach. This experiment has been modelled with the Conditional Moment Closure (CMC) model [16] in RANS [17–19] or LES [20]. The transported PDF model was also employed with LES [21,22] and a DNS was conducted [23]. None of the above-mentioned studies considered non-adiabatic conditions, i.e., radiative and convective heat transfer from the flow to the surrounding walls, nor the variability of inlet conditions.

This work presents a methodology based on the Incompletely Stirred Reactor Network (ISRN) formulation [24,25] and on surrogate modelling to quantify autoignition stochasticity accurately and with a low computational cost. The stochastic modelling is performed for the autoignition experiment of Ref. [13] by considering uncertainties in three input conditions and a surrogate model trained on several ISRN simulations of the burner. The PDFs of the autoignition spot locations are then computed by querying the trained surrogate model via Monte Carlo sampling of the random input quantities and eventually compared with the experimental data.

2. Experimental dataset

The hydrogen autoignition experiments performed by Markides and Mastorakos [13] are the focus of the current work. In the experiments, H_2 was diluted with N_2 and injected into a turbulent co-flow of heated air (see Fig. 1). The fuel nozzle had a 2.24 mm diameter (d). The inner burner diameter was 24.8 mm ($2R$). Air was electrically preheated and flowed into a circular quartz tube after passing through a perforated plate to promote turbulence. The fuel nozzle was located 63 mm downstream of the perforated plate to allow turbulence to develop. Co-flow air velocities (U_{ox}) up to 35 m/s, with temperatures (T_{ox}) up to 1015 K, were achieved. The fuel mixture composition by mass was $Y_{H_2} = 0.13$ and $Y_{N_2} = 0.87$. A certain amount of fuel preheating was unavoidable due to heat transfer from the hot co-flowing air. Thus, T_f was not an independent parameter, but depended on the air temperature (T_{ox}) and the mixture flow rate and composition [13].

Hot wire and acetone Planar Laser-Induced Fluorescence (PLIF) measurements were performed to understand the mixing field at the following conditions: $T_f = T_{ox} = 473$ K and $U_f = U_{ox} = 7$ m/s [26]. These conditions exhibited dynamic similarity with the "hot" autoignition runs [27]. The axial velocity field was characterised with a 1.25 mm long, 5 μm diameter hot wire and a Dantec Constant Temperature Anemometer (CTA) system, whereas the mixture fraction field was obtained by suitably normalising the PLIF measurements of the local volumetric (or molar) concentration of injected fluorescent-laden acetone. A comprehensive description of the hot wire and PLIF measurements can be found in Refs. [14,15,26,27].

Please cite this article as: S. Iavarone, S. Gkantonas and E. Mastorakos, Stochastic low-order modelling of hydrogen autoignition in a turbulent non-premixed flow, Proceedings of the Combustion Institute, https://doi.org/10.1016/j.proci.2022.07.129

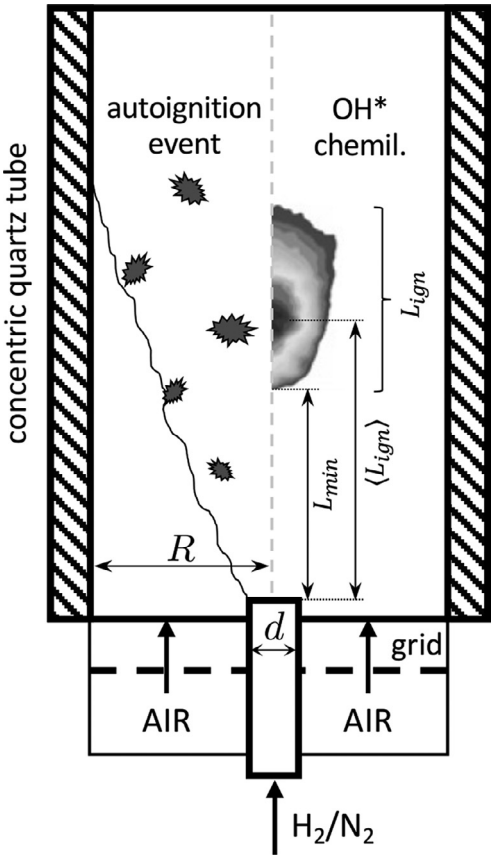

Fig. 1. Apparatus schematic (not to scale) with indication of autoignition events (left) and representative averaged OH* chemiluminescence contour (right) [13].

In the experiments, fuel velocities (U_f) ranged from 20 to 120 m/s, with temperatures (T_f) between 650 K and 930 K [13]. Up to 2000 OH* chemiluminescence images per operating condition (set of T_{ox}, U_{ox}, T_f, and U_f) were taken and the statistics of the autoignition spot axial location, L_{ign}, was determined (see Fig. 1). The PDF of L_{ign} gave two different quantities, i.e., mean and minimum autoignition lengths, denoted as $\langle L_{ign} \rangle$ and $L_{\min}$, respectively, with $L_{\min}$ defined as the axial distance where the PDF reached 3% of its peak value. An absolute systematic uncertainty of ±5% was estimated for all reported spot locations. Instantaneous measurements of T_{ox} were performed, and their PDF was found to closely follow a normal distribution, with measured RMS reaching values up to 2.0 K at the investigated conditions. Some of this spread is due to the finite precision of the instrument, but some is due to heat losses and boundary layers. It is of interest to know to what extent the PDF(T_{ox}) determines the PDF(L_{ign}) and to replicate the stochasticity of autoignition due to parameter fluctuations. The focus of this work is to present a methodology that can achieve such purposes with high accuracy and low computational effort.

3. Methodology for stochastic modelling

Fig. 2 depicts the framework of the methodology adopted in this work to replicate the stochasticity of autoignition kernel locations reported in the experiments. Three random input parameters were considered, namely the co-flow air temperature (T_{ox}), the fuel temperature (T_f), and the average temperature of the quartz glass wall (T_w). Performing a Monte Carlo sampling of the three quantities and a CFD simulation (with or without the ISRN approach) for each sampled combination to obtain a distribution of autoignition lengths would be computationally unfeasible. To overcome this computational barrier, a space-filling design was generated over the three-dimensional parameter space via the Latin Hypercube Sampling method [28], which significantly reduces the number of sampled points compared to Monte Carlo methods. ISRN runs were performed for each sampled combination on top of an inert flow solution provided by a non-reactive LES. For the problem of autoignition, where only small density changes are expected to occur before autoignition happens, post-processing non-reacting flow mixing patterns introduces only small errors [1]. Moreover, the ISRN computations were carried out on the same mixing field since changes in the input conditions were considered small enough to cause negligible differences in the mixing field. A surrogate model (also called meta-model or response surface) was trained on the autoignition lengths obtained from the ISRN simulations. Once an accurate surrogate model had been obtained, a crude Monte Carlo sampling of the PDFs of the input parameters was performed. Three normal distributions were assumed for T_{ox}, T_f, and T_w, having the same standard deviation $\sigma = 2$ K. Thus, the assumed distribution of T_{ox} closely followed the measured one. The random samples of the three parameters were fed to the surrogate model to obtain the PDF of autoignition lengths and compute the minimum and mean values, which are then compared with the experimental data. The numerical setup of the LES runs is described in Section 3.1, whereas the details of the ISRN methodology are presented in Sections 3.2 and 3.3.

3.1. Non-reactive CFD simulations

In this work, the mixing field was provided by a non-reactive LES. The LES equations for mass, momentum, energy and mixture fraction were solved for this burner using the software CONVERGE [29]. The sub-grid scale stress tensor was modelled with the dynamic Smagorinsky model [30]. To extract more information about the

Please cite this article as: S. Iavarone, S. Gkantonas and E. Mastorakos, Stochastic low-order modelling of hydrogen autoignition in a turbulent non-premixed flow, Proceedings of the Combustion Institute, https://doi.org/10.1016/j.proci.2022.07.129

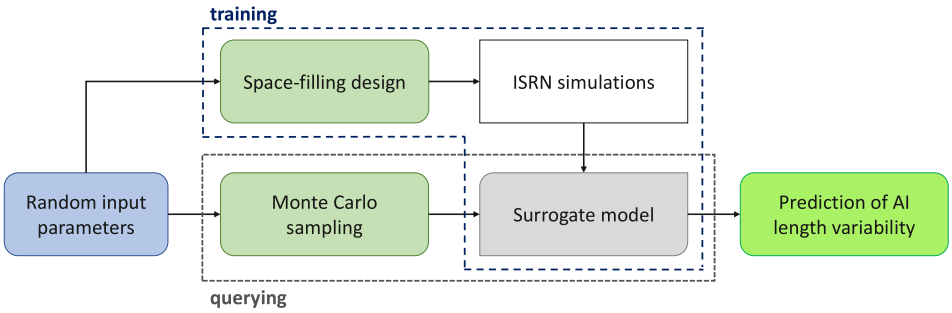

Fig. 2. Methodology scheme. The tasks involved in the training of the surrogate model and its successive querying via Monte Carlo sampling are indicated.

mixing field, the sub-grid scale mixture fraction variance was expressed as $\widetilde{\xi''^2} = c_v \Delta^2 \nabla\widetilde{\xi} \cdot \nabla\widetilde{\xi}$ with $c_v = 0.1$ [31] and the filter width Δ calculated as the cube root of the LES cell volume, similar to Ref. [32]. In addition, the scalar dissipation rate $\widetilde{N}$ was computed considering both resolved and sub-grid scale contributions, i.e., $\widetilde{N} = \widetilde{N}_{res} + \widetilde{N}_{sgs}$, in which $\widetilde{N}_{res} = D\nabla\widetilde{\xi} \cdot \nabla\widetilde{\xi}$ and $\widetilde{N}_{sgs} = \frac{c_N}{2}\frac{\mu_t}{\tilde{\rho}\Delta^2}\widetilde{\xi''^2}$ with $c_N = 42$ [33]. D is the molecular diffusivity, μ_t is the turbulent viscosity and $\tilde{\rho}$ is the filtered density. The closures for mixture fraction variance and scalar dissipation rate were implemented as User-Defined Functions in CONVERGE. The pressure implicit with splitting of operator (PISO) scheme and an implicit first-order temporal scheme were employed for solving the governing equations of the flow. The experimental velocity profiles were imposed at both fuel and air inlets along with Dirichlet boundary conditions for scalars and pressure. At the outlet, zero-gradient boundary conditions were enforced for velocity components and scalars and the pressure was fixed to atmospheric. No-slip conditions were used at the walls, assumed adiabatic at an imposed temperature. A digital filter was used for synthetic turbulence with intensity $I = 0.15$ and integral length scale $L_t = 0.004$ m. The turbulent Schmidt number Sc_t was set to 0.4. Adaptive Mesh Refinement with minimum cell size $\delta = 0.125$ mm was employed, resulting in a total number of cells ≈ 2.5M.

3.2. The ISRN approach

In CMC, transport equations are solved for the conditionally averaged reacting scalars, Q, which are conditioned on the mixture fraction, ξ. Particularly, $Q = \langle \phi | \xi(\mathbf{x}, t) = \eta \rangle$, where ϕ is a generic reacting scalar and η is a sample space variable for the mixture fraction ξ. It is common practice to use a dual mesh approach, where the CMC grid is coarser than the LES one. Assuming steady-state and neglecting turbulent transport in the longitudinal direction by conditional fluctuations, i.e., thin-shear flow, the CMC shear flow equations can be obtained from the canonical form of the CMC equations by averaging across the flow [16]. The present formulation accounts for non-unity Lewis numbers, and thus the governing equations for the i-th conditionally averaged species mass fraction, Q_i, and the conditionally averaged enthalpy, Q_h, can be written as

$$U_\eta^* \frac{\partial Q_i}{\partial z} = \langle \dot{\omega}_i | \eta \rangle + \frac{Le_\xi}{Le_i} N_\eta^* \frac{\partial^2 Q_i}{\partial \eta^2} + \left(\frac{Le_\xi}{Le_i} - 1 \right) M_\eta^* \frac{\partial Q_i}{\partial \eta}, \tag{1}$$

$$\begin{aligned} U_\eta^* \frac{\partial Q_h}{\partial z} = {} & \langle \dot{\xi} | \eta \rangle + Le_\xi N_\eta^* \frac{\partial^2 Q_h}{\partial \eta^2} \\ & + \sum_{i=1}^{N} \left(\frac{1}{Le_i} - 1 \right) Le_\xi N_\eta^* \frac{\partial Q_i}{\partial \eta} \frac{\partial Q_{h,i}}{\partial \eta} \\ & + \sum_{i=1}^{N} \left(\frac{1}{Le_i} - 1 \right) Le_\xi N_\eta^* \frac{\partial^2 Q_i}{\partial \eta^2} Q_{h,i} \\ & + \sum_{i=1}^{N} \left(\frac{1}{Le_i} - 1 \right) Le_\xi M_\eta^* \frac{\partial Q_i}{\partial \eta} Q_{h,i}, \end{aligned} \tag{2}$$

where the terms including the i-th species Lewis number, Le_i, must be considered to capture differential diffusion. In particular, non-unity Lewis numbers were considered only for H-atom and H_2, i.e., $Le_H = 0.18$ and $Le_{H_2} = 0.3$, as in Ref. [34]. Le_ξ is the Lewis number for the mixture fraction and is assumed equal to unity. The inert species, i.e., N_2, is not transported via Eqs. 1–2 to ensure that mass and enthalpy are conserved. A star, *, denotes the cross-stream average of the quantity ϕ defined as

$$\phi_\eta^* = \frac{\{\phi_\eta P_\eta\}}{\{P_\eta\}} = \frac{\lim_{R\to\infty} \int_{r\le R} \phi_\eta P_\eta r dr}{\lim_{R\to\infty} \int_{r\le R} P_\eta r dr}, \tag{3}$$

where the subscript η indicates conditioning on the mixture fraction, i.e., η is the sample space variable of the mixture fraction, $\phi_\eta = \langle \phi | \eta \rangle$, and $P_\eta \equiv P(\eta)$ is the PDF of the mixture fraction. The equations above can be seen as the 1D equivalent of the

Please cite this article as: S. Iavarone, S. Gkantonas and E. Mastorakos, Stochastic low-order modelling of hydrogen autoignition in a turbulent non-premixed flow, Proceedings of the Combustion Institute, https://doi.org/10.1016/j.proci.2022.07.129

ISRN approach presented by Gkantonas et al. [24]. Instead of dealing with volume-averaged quantities, this formulation is based on cross-stream averaging and represents a series of Incompletely Stirred Reactors (ISRs) that bears some similarity with a plug flow reactor approximation including micro-mixing effects. A similar approach has also been proposed in Ref. [25]. The CFD-derived quantities needed for the ISRN simulations are the mean velocity vector, density, mean mixture fraction, mixture fraction variance and mean scalar dissipation rate. When extracted from an LES, the instantaneous quantities should be time-averaged, so that information about the mean flow and mixing fields is fed to the ISRN. In Eqs. 1–3, P_η was modelled as a clipped-Gaussian PDF and N_η was calculated from the AMC model [35]. M_η^* was calculated by cross-stream averaging (Eq. 3) the conditionally filtered diffusion term M_η, modelled here as

$$M_\eta = \frac{1}{\rho P_\eta}\frac{\partial}{\partial \eta}(\rho P_\eta N_\eta), \tag{4}$$

according to Ref. [16]. In Eq. 2, the term $\langle \dot{\zeta}|\eta\rangle$ accounts for the convective and radiative heat transfer from the gaseous phase to the quartz tube. The convective part was modelled according to Hergart and Peters [36]

$$\langle \dot{\zeta}_{conv}|\eta\rangle = \alpha(Q_T - T_w), \tag{5}$$

where T_w is the quartz wall temperature, and α is defined as

$$\alpha = \frac{hA(T - T_w)}{\int_0^1 (Q_T - T_w)P_\eta d\eta}, \tag{6}$$

with h being the heat transfer coefficient, A the wall area, T_w the wall temperature and T the unconditional fluid temperature. The radiative part was calculated based on an optically thin assumption and the RADCAL model previously applied to CMC [37].

3.3. Numerical settings

An operator splitting technique was implemented for the solution of the ISRN equations, which were advanced in time with a constant (pseudo) time-step $\Delta t = 10^{-6}$ s until steady-state was reached. Transport in physical space, i.e., the first terms of Eqs. 1–2, was solved first, followed by transport in mixture fraction space and chemical source term integration. The tridiagonal matrix algorithm (TDMA) was employed for the transport in physical space and the micromixing terms. The chemical source term was closed with a first-order approximation, and the integration was executed by the SpeedCHEM chemistry solver employing an analytical Jacobian formulation. The kinetic mechanism by Hong et al. [38], which provided good ignition delay times of hydrogen [39], was employed. It consists of 10 species and 31 reactions. A second-order central difference scheme was adopted for the second-order derivatives in mixture fraction space and an upwind scheme for the derivatives in physical space. The mixture fraction space was discretised using 101 bins clustered around the stoichiometric mixture fraction ($\xi_{st} = 0.184$) with sufficient resolution around the most reactive mixture fraction. The latter was obtained from standalone homogeneous mixture calculations following the initialisation procedure in Ref. [1], and ranged from 0.034 to 0.048 in the current configuration. The absolute enthalpy equation was solved and the temperature was calculated from species and enthalpy with absolute tolerance 10^{-8}. The heat transfer through the outer quartz tube was considered in the simulations and a constant and uniform temperature was assumed. An estimate of this average temperature was obtained off-line via a conjugate heat transfer calculation that considers convection from the inert gas to the quartz pipe wall, 1D conduction within the wall, and radiation from the wall towards the surroundings. A quasi-steady state assumption was made for the inert gas, with temperature values matching an experimental profile measured inside the pipe, and a conduction-source equation was solved for the solid to compute the final wall temperature.

The "equal velocity" experimental case, where the mean inlet velocities of fuel and air streams are identical, $U_f = U_{ox} = 26$ m/s, was targeted. An interval of values were reported in the experimental campaign for the inlet fuel and air temperatures. A fuel temperature $T_f = 750$ K was considered in accordance with other numerical works [17,18,21,22].

4. Results

The ISRN equations were solved in post-processing on top of the inert mixing field resolved by LES. The validation of the LES was performed by comparing simulated profiles of velocity, mixture fraction and mixture fraction variance with the corresponding hot wire and acetone PLIF measurements. Fig. 3 shows a comparison of experimental and simulated radial and axial profiles, which indicates that the simulation can capture the inert mixing field with satisfying accuracy.

The behaviour of the reacting flow at the nominal conditions of the "equal velocity" experimental case, i.e., $U_f = U_{ox} = 26$ m/s and $T_f = 750$ K, was then targeted by the ISRN simulations. The co-flow air temperature T_{ox} ranged from 950 to 975 K, while a fixed value of the average wall temperature, $T_w = 675$ K, was considered. The autoignition length was defined based on the OH-radical, at the location of the maximum gradient of the OH-radical mass fraction. Little difference with OH*, H, O or T were observed. The hydrogen autoignition length is well captured, as shown in Fig. 4, demonstrating that the ISRN approach can provide accurate predictions of autoignition. Particularly, the ISRN

Please cite this article as: S. Iavarone, S. Gkantonas and E. Mastorakos, Stochastic low-order modelling of hydrogen autoignition in a turbulent non-premixed flow, Proceedings of the Combustion Institute, https://doi.org/10.1016/j.proci.2022.07.129

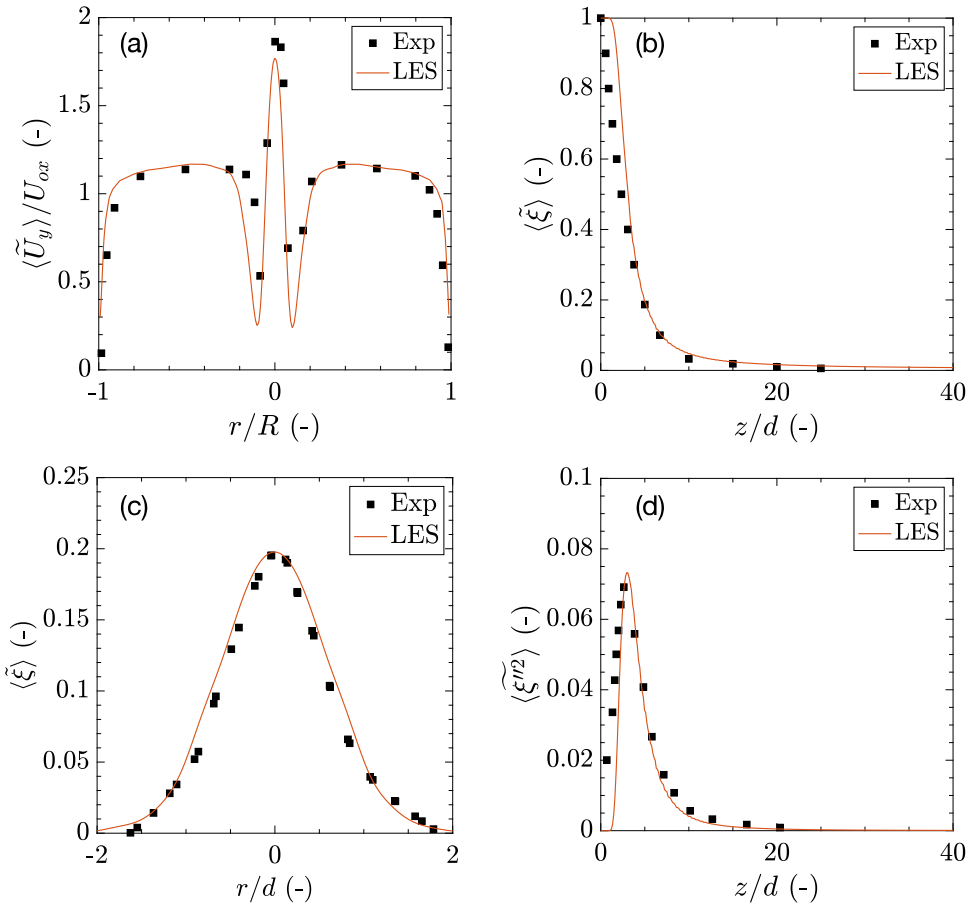

Fig. 3. Experiments (symbols) and simulations (lines): mean radial profiles of axial velocity $\langle \widetilde{U}_y \rangle$ (normalised by the bulk velocity, U_{ox}) and mixture fraction $\langle \widetilde{\xi} \rangle$ at $y = 2$ mm (a-c); mean axial profiles of $\langle \widetilde{\xi} \rangle$ and mixture fraction variance $\langle \widetilde{\xi''^2} \rangle$ along the centreline (b-d).

approach, carried out at the nominal experimental conditions (e.g., nominal T_{ox} values), can predict the mean autoignition lengths $\langle L_{ign} \rangle$, as shown in Fig. 4. To capture the minimum autoignition lengths $L_{\min}$, one needs to account for the fluctuations of the autoignition kernel locations due to the fluctuations of the input conditions. Thus, a stochastic approach is needed, and it is enabled by using a surrogate model.

The space-filling design was generated within the following ranges of variability of the input parameters T_f, T_{ox}, and T_w: 650–800 K, 920–1000 K and 580–720 K, respectively. A total of 100 different combinations were sampled from the parameter space via Latin Hypercube Sampling, and hence 100 ISRN simulations were performed. The simulations took about 36 hours to run over 20 processors in parallel. Only 66 out of 100 simulations resulted in autoignition. A response surface for L_{ign} was trained over the 66 ISRN runs providing autoignition. The chosen response surface is a Gaussian Process (GP) with Matérn 5/2 kernel [40], which was trained in MATLAB with its accuracy evaluated during training by 5-fold cross validation. Gaussian Process (or kriging) is an interpolation method where the input-output relationship is expressed by a combination of a trend function and a residual term [40]:

$$y(\mathbf{x}) = \mu(\mathbf{x}) + z(\mathbf{x}) = \sum_{i=0}^{p} \beta_i f_i(\mathbf{x}) + \mathrm{GP}(\mathbf{x}, \boldsymbol{\theta}) \quad (7)$$

The trend function $\mu(\mathbf{x})$ is a weighted linear combination of $p+1$ polynomials, with weights β_i determined by generalised least squares. The subscript i also indicates the degree of the polynomials $f_i(\mathbf{x})$. The residual function $z(\mathbf{x})$ is expressed by a Gaussian process, i.e., a normal distribution, $\mathrm{GP}(\mathbf{x}, \boldsymbol{\theta}) = \mathcal{N}(0, K(\mathbf{x}, \boldsymbol{\theta}))$, having a specific covariance function (kernel) K with a set hyperparameters $\boldsymbol{\theta}$ determined by maximum likelihood estimation [41]. The residual function creates a localised

Please cite this article as: S. Iavarone, S. Gkantonas and E. Mastorakos, Stochastic low-order modelling of hydrogen autoignition in a turbulent non-premixed flow, Proceedings of the Combustion Institute, https://doi.org/10.1016/j.proci.2022.07.129

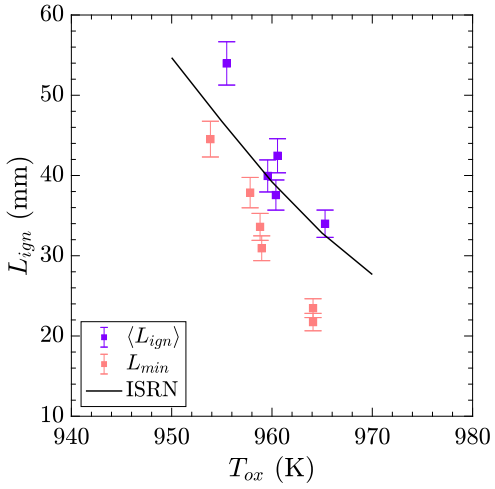

Fig. 4. Autoignition lengths for hydrogen at different inlet air temperatures T_{ox}: minimum $L_{\min}$ and mean $\langle L_{ign} \rangle$ from experiments and L_{ign} predicted by ISRN.

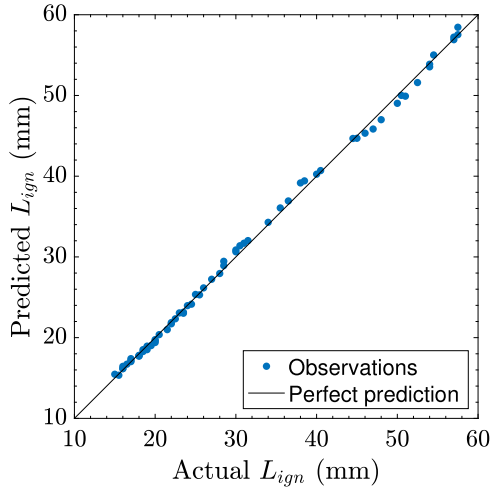

Fig. 5. Parity plot of autoignition lengths for hydrogen, L_{ign}, obtained by the ISRN simulations and predicted by the GP.

deviation by weighting the points in the training set $\mathbf{x}_d$ that are closer to the target points $\mathbf{x}_t$. Other approaches, such as neural networks, support vector machines, or polynomials, may have been used as surrogates. The latter two were considered in the training stage but they did not provide an accurate fitting as the GP. The training of the GP was performed in less than one minute on a 4-core laptop. Fig. 5 shows the parity plot of the L_{ign} values obtained by the ISRN simulations and the GP. The low-order model fits the L_{ign} values with great accuracy. The maximum discrepancy between the values provided by the ISRN runs and obtained by the surrogate model is 1.16 mm.

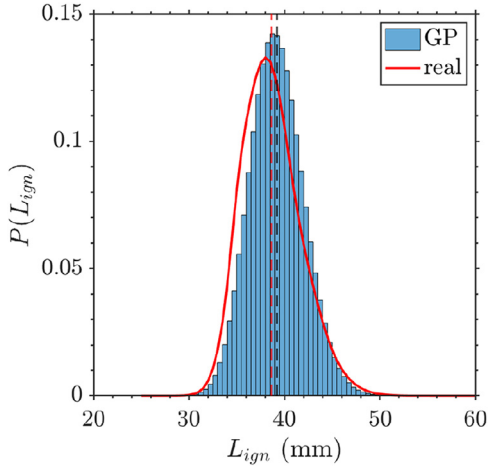

Fig. 6. Histogram of the PDF(L_{ign}) obtained by the GP when propagating the variability of only one input quantity, T_{ox}. The *real* PDF of L_{ign} is depicted by a red solid line. The black and red dashed vertical lines indicate the means for GP and real PDFs, respectively. (For interpretation of the references to colour in this figure legend, the reader is referred to the web version of this article.)

Prior to using it for propagating the uncertainty of the three input parameters on the autoignition length, the GP was first assessed in its capability to replicate the PDFs of L_{ign} when the PDF of one of the input quantities is supposedly known. A total of 21 ISRN simulations were performed at fixed $T_f = 750$ K and $T_w = 675$ K, while T_{ox} was varied from 950 K to 970 K to sample a hypothetical normal distribution with mean $\mu = 960$ K and standard deviation $\sigma = 2$ K, namely, $T_{ox} = \mathcal{N}(960, 2)$. A one-to-one correspondence between the PDFs of T_{ox} and L_{ign} exists in this case, and a surrogate model must be able to provide a good estimation of the PDF of L_{ign}, its mean and standard deviation. The PDF of L_{ign} was computed by querying the trained GP 10^8 times. The 10^8 GP evaluations were obtained in less than 4 minutes on a 4-core laptop. A fairly good agreement can be seen in Fig. 6 between the PDF known a priori and the one computed by the surrogate, considering that the GP was not trained on the ISRN data used for this test. Also, a higher number of training samples can be employed to improve the response surface fitting and increase the accuracy of the GP for *unseen* data. Training the GP on only 66 simulations already provide good enough accuracy for L_{ign} since the mean and standard deviation computed by the GP are 39.2 mm and 2.8 mm, whereas the analytical values, obtained from the numerical integration of the *real* PDF of L_{ign}, are 38.6 mm and 3.1 mm. The mean values are indicated in Fig. 6 by black and red dashed vertical lines for GP and real PDFs, respectively. The same mean and standard deviation

Please cite this article as: S. Iavarone, S. Gkantonas and E. Mastorakos, Stochastic low-order modelling of hydrogen autoignition in a turbulent non-premixed flow, Proceedings of the Combustion Institute, https://doi.org/10.1016/j.proci.2022.07.129

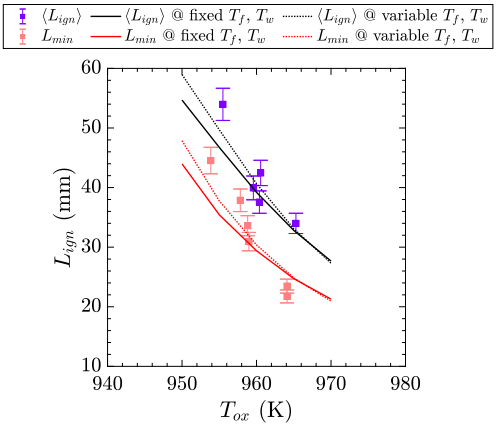

Fig. 7. $L_{\min}$ and $\langle L_{ign}\rangle$ from experiments (symbols with error bars) and predicted by the GP at fixed mean values of T_f and T_w (solid lines) and at variable mean values of T_f and T_w (dotted lines).

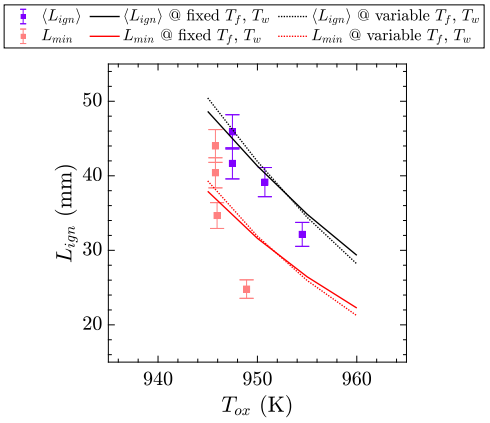

Fig. 8. $U_f = U_{ox} = 20$ m/s case: $L_{\min}$ and $\langle L_{ign}\rangle$ from experiments (symbols with error bars) and predicted by the GP at fixed mean values of T_f and T_w (solid lines) and at variable mean values of T_f and T_w (dotted lines).

values were obtained by considering 10^7 GP evaluations.

At the Monte Carlo sampling stage, three normal PDFs were assumed for T_{ox}, T_f, and T_w, having the same standard deviation $\sigma = 2$ K. The mean values for T_f and T_w were assumed to be the nominal ones, i.e., $T_f = 750$ K and $T_w = 675$ K. The mean value of T_{ox} was varied from 950 K to 975 K to comply with the range at which the experimental data were available. 10^7 combinations were randomly sampled from the joint PDF of the three input quantities. The autoignition length PDF was obtained from the GP evaluations at the input random samples. Minimum, $L_{\min}$, and mean, $\langle L_{ign}\rangle$, autoignition lengths were obtained from the PDF(L_{ign}) and compared with the experimental data in Fig. 7. The solid lines in Fig. 7 depict $L_{\min}$ and $\langle L_{ign}\rangle$ profiles obtained while keeping the mean T_f and T_w at their nominal values. A fairly good agreement can be noticed. However, in the experiment, because of convective heat transfer from the injection pipe walls, T_f is not an independent parameter but a function of T_{ox}, U_{ox}, and U_f. Also, T_w is uncertain and depends on T_{ox} and U_{ox}. Considering the mean values of T_f and T_w in the ranges 720–760 K and 600–680 K, respectively, and both monotonically increasing with T_{ox}, the dotted lines in Fig. 7 were obtained. A closer agreement between experimental and simulated values of $\langle L_{ign}\rangle$ and $L_{\min}$ can be observed in this case.

The use of a surrogate model enables a Global Sensitivity Analysis (GSA) through Sobol indices [42], which are computed for each stochastic model parameter and highlight their fractional contribution to the output quantity variance. This contribution is estimated by the following *first-order* or *main effect* Sobol index:

$$S_i = \frac{V_{X_i}(E_{X_{\sim i}}(\mathcal{M}(\boldsymbol{X})|X_i))}{V(\mathcal{M}(\boldsymbol{X}))}, \tag{8}$$

where $\boldsymbol{X}$ is the set of random variables, $V(\mathcal{M}(\boldsymbol{X}))$ is the total variance of the model response $\mathcal{M}(\boldsymbol{X})$, and the numerator represents the variance determined by the i-th variable, calculated with respect to an expected value of the model response. The latter is obtained by varying all the random variables within their uncertainty ranges but the i-th one, kept constant. As thousands of runs are required to get accurate indices, the use of a surrogate model makes GSA computationally feasible. The indices were then computed and reported as follows for the input parameters: 0.980 for T_{ox}, 0.013 for T_f, and and 0.004 for T_w. Their sum is equal to one minus the values of higher-order interaction indices, neglected here. The indices show that the autoignition length variability is mainly caused by the inlet co-flow temperature. This can be explained by the fact that in the studied flow, the most reactive mixture fraction, which is crucial for autoignition [1], is overall very lean. Thus, the location of the autoignition kernels L_{ign} is less susceptible to changes due to T_f but strongly affected by T_{ox}. Although the variability of the inlet fuel temperature and the average wall temperature is not impactful on the autoignition length variance, their nominal values are and determine different final values of $\langle L_{ign}\rangle$ and $L_{\min}$, as can be seen by comparing solid and dotted lines in Fig. 7.

Finally, the same methodology described above was applied to another "equal velocity" case, i.e., $U_f = U_{ox} = 20$ m/s. Fig. 8 shows the comparison of experimental and simulated profiles of $L_{\min}$ and $\langle L_{ign}\rangle$. The values are well predicted by the joint ISRN-surrogate modelling approach, apart from

Please cite this article as: S. Iavarone, S. Gkantonas and E. Mastorakos, Stochastic low-order modelling of hydrogen autoignition in a turbulent non-premixed flow, Proceedings of the Combustion Institute, https://doi.org/10.1016/j.proci.2022.07.129

the value of $L_{\min}$ at $T_{ox} = 950$ K, which is overestimated. The GP model can be trained also for cases where U_f is different from U_{ox}. The accuracy of the GP, or any other surrogate model, in predicting stochastic autoignition events is strongly related to that of the training simulation data. Particularly, the ISRN approach needs to capture the variation of the mean autoignition length $\langle L_{ign} \rangle$ with the nominal input parameters correctly to enable the successful application of the joint ISRN-surrogate modelling approach to a different case. The validation of ISRN to jet in coflow and crossflow configurations is left for future studies.

5. Summary and conclusions

A novel approach using Incompletely Stirred Reactor Network (ISRN) modelling and surrogate modelling for stochastic estimation of non-premixed autoignition in turbulent flames has been presented. The model has been applied to an experiment with hydrogen continuously injected in a confined turbulent co-flow of preheated air, for which experimental measurements of the fluctuations of inlet parameters and autoignition spot location are available. The ISRN method solves the CMC shear flow equations in post-processing on top of an inert flow LES, thus significantly reducing the computational costs. The effect of non-adiabatic conditions and differential diffusion have been included. The approach captured well the mean autoignition lengths measured in the experiments. This newly validated simulation tool for autoignition reduces the computational costs with minimal loss of accuracy, ensuring the exploration of multidimensional parameter spaces for UQ, optimization, and sensitivity analysis. In this work, the fluctuations of three input quantities, i.e., inlet fuel and air temperatures, and average outer tube temperature, were considered to predict the variability of the autoignition lengths observed during the experiments. The assumed input variability was propagated to estimate the mean and minimum flame liftoff locations. A total of 100 ISRN simulations of the burner were performed at input parameter combinations sampled via a space-filling design. A Gaussian Process was chosen as a surrogate model and trained on the ISRN simulations. The accuracy of the surrogate was tested on a dataset not used for its training. The final quantification of the autoignition locations was achieved by querying the surrogate model via Monte Carlo sampling (10^7 points) of the selected random input quantities. Fast and accurate predictions of minimum and mean autoignition lengths were obtained.

The methodology presented in this proof-of-concept study has quantified the stochasticity of autoignition locations in an efficient and computationally feasible way. It can be used effectively to determine the sensitivity of autoignition to the fluctuations of inlet parameters. Such analyses are critical to the design of practical systems like premixers of aero-derivative gas turbines and become especially relevant for high pressures and the expected switch to hydrogen combustion.

Declaration of Competing Interest

The authors declare that they have no known competing financial interests or personal relationships that could have appeared to influence the work reported in this paper.

Acknowledgements

The research leading to these results has received funding from the European Union's Horizon 2020 research and innovation programme under the CoEC project, grant agreement No 952181, and from Siemens Energy. This work used the ARCHER UK National Supercomputing Service (http://www.archer.ac.uk).

References

[1] E. Mastorakos, Ignition of turbulent non-premixed flames, Prog. Energy Combust. Sci. 35 (1) (2009) 57–97.
[2] C. Xiouris, T. Ye, J. Jayachandran, F. Egolfopoulos, Laminar flame speeds under engine-relevant conditions: uncertainty quantification and minimization in spherically expanding flame experiments, Combust. Flame 163 (2016) 270–283.
[3] Y. Zhang, M. Jeanson, R. Mével, Z. Chen, N. Chaumeix, Optimizing mixture properties for accurate laminar flame speed measurement from spherically expanding flame: application to $H_2/O_2/N_2$/He mixtures, Combust. Flame 231 (2021) 111487.
[4] J. Prager, H. Najm, K. Sargsyan, C. Safta, W. Pitz, Uncertainty quantification of reaction mechanisms accounting for correlations introduced by rate rules and fitted arrhenius parameters, Combust. Flame 160 (9) (2013) 1583–1593.
[5] W. Ji, J. Wang, O. Zahm, Y. Marzouk, B. Yang, Z. Ren, C. Law, Shared low-dimensional subspaces for propagating kinetic uncertainty to multiple outputs, Combust. Flame 190 (2018) 146–157.
[6] A. Tomlin, The use of global uncertainty methods for the evaluation of combustion mechanisms, Reliab. Eng. Syst. Saf. 91 (10) (2006) 1219–1231.
[7] I.G. Zsély, J. Zádor, T. Turányi, Uncertainty analysis of NO production during methane combustion, Int. J. Chem. Kinet. 40 (11) (2008) 754–768.
[8] A.C. Lipardi, P. Versailles, G.M. Watson, G. Bourque, J.M. Bergthorson, Experimental and numerical study on NO_x formation in CH_4–air mixtures diluted with exhaust gas components, Combust. Flame 179 (2017) 325–337.
[9] M.-S. Oh, J.O. Berger, Adaptive importance sampling in monte carlo integration, J. Stat. Comput. Simul. 41 (3–4) (1992) 143–168.

Please cite this article as: S. Iavarone, S. Gkantonas and E. Mastorakos, Stochastic low-order modelling of hydrogen autoignition in a turbulent non-premixed flow, Proceedings of the Combustion Institute, https://doi.org/10.1016/j.proci.2022.07.129

[10] F. Bouchet, J. Rolland, J. Wouters, Rare event sampling methods, Chaos 29 (8) (2019) 080402.
[11] T. Ziehn, A.S. Tomlin, A global sensitivity study of sulfur chemistry in a premixed methane flame model using HDMR, Int. J. Chem. Kinet. 40 (11) (2008) 742–753.
[12] H.N. Najm, Uncertainty quantification and polynomial chaos techniques in computational fluid dynamics, Annu. Rev. Fluid Mech. 41 (1) (2009) 35–52.
[13] C. Markides, E. Mastorakos, An experimental study of hydrogen autoignition in a turbulent co-flow of heated air, Proc. Combust. Inst. 30 (1) (2005) 883–891.
[14] C. Markides, G. De Paola, E. Mastorakos, Measurements and simulations of mixing and autoignition of an n-heptane plume in a turbulent flow of heated air, Exp. Therm. Fluid Sci. 31 (5) (2007) 393–401.
[15] C. Markides, E. Mastorakos, Experimental investigation of the effects of turbulence and mixing on autoignition chemistry, Flow Turbul. Combust. 86 (3) (2011) 585–608.
[16] A. Klimenko, R. Bilger, Conditional moment closure for turbulent combustion, Prog. Energy Combust. Sci. 25 (6) (1999) 595–687.
[17] S. Patwardhan, K. Lakshmisha, Autoignition of turbulent hydrogen jet in a coflow of heated air, Int. J. Hydrog. Energy 33 (23) (2008) 7265–7273.
[18] A.J.M. Buckrell, C.B. Devaud, Investigation of mixing models and conditional moment closure applied to autoignition of hydrogen jets, Flow Turbul. Combust. 90 (3) (2013) 621–644.
[19] S. Navarro-Martinez, A. Kronenburg, Flame stabilization mechanisms in lifted flames, Flow Turbul. Combust. 87 (2) (2011) 377–406.
[20] I. Stanković, A. Triantafyllidis, E. Mastorakos, C. Lacor, B. Merci, Simulation of hydrogen auto-ignition in a turbulent co-flow of heated air with les and cmc approach, Flow Turbul. Combust. 86 (3) (2011) 689–710.
[21] W. Jones, S. Navarro-Martinez, O. Röhl, Large eddy simulation of hydrogen auto-ignition with a probability density function method, Proc. Combust. Inst. 31 (2) (2007) 1765–1771.
[22] W. Jones, S. Navarro-Martinez, Study of hydrogen auto-ignition in a turbulent air co-flow using a large eddy simulation approach, Comput. Fluids 37 (7) (2008) 802–808.
[23] S.G. Kerkemeier, C.N. Markides, C.E. Frouzakis, K. Boulouchos, Direct numerical simulation of the autoignition of a hydrogen plume in a turbulent coflow of hot air, J. Fluid Mech. 720 (2013) 424–456.
[24] S. Gkantonas, J. Foale, A. Giusti, E. Mastorakos, Soot emission simulations of a single sector model combustor using incompletely stirred reactor network modeling, J. Eng. Gas Turbines Power 142 (10) (2020) 101007.
[25] S. Gkantonas, Predicting soot emissions with advanced turbulent reacting flow modelling, University of Cambridge, UK, 2021 Ph.D. thesis.
[26] C.N. Markides, Autoignition in Turbulent Flows, University of Cambridge, 2005 Ph.D. thesis.
[27] C.N. Markides, E. Mastorakos, Flame propagation following the autoignition of axisymmetric hydrogen, acetylene, and normal-heptane plumes in turbulent coflows of hot air, J. Eng. Gas Turbines Power 130 (1) (2007) 011502-2.
[28] M.D. McKay, R.J. Beckman, W.J. Conover, Comparison of three methods for selecting values of input variables in the analysis of output from a computer code, Technometrics 21 (2) (1979) 239–245.
[29] K. Richards, P. K. Senecal, E. Pomraning, Converge 3.0; Convergent Science: Madison, WI, USA, 2021.
[30] M. Germano, U. Piomelli, P. Moin, W.H. Cabot, A dynamic subgrid scale eddy viscosity model, Phys. Fluids 3 (1990) 1760–1765.
[31] C.D. Pierce, P. Moin, A dynamic model for subgrid-scale variance and dissipation rate of a conserved scalar, Phys. Fluids 10 (12) (1998) 3041–3044.
[32] H. Zhang, A. Giusti, E. Mastorakos, LES/CMC modelling of ignition and flame propagation in a non-premixed methane jet, Proc. Combust. Inst. 37 (2) (2019) 2125–2132.
[33] A. Garmory, E. Mastorakos, Capturing localised extinction in Sandia flame F with LES–CMC, Proc. Combust. Inst. 33 (1) (2011) 1673–1680.
[34] M.-C. Ma, C.B. Devaud, A conditional moment closure (CMC) formulation including differential diffusion applied to a non-premixed hydrogen–air flame, Combust. Flame 162 (1) (2015) 144–158.
[35] E. O'Brien, T. Jiang, The conditional dissipation rate of an initially binary scalar in homogeneous turbulence, Phys. Fluids A Fluid Dyn. 3 (12) (1991) 3121–3123.
[36] C. Hergart, N. Peters, Applying the representative interactive flamelet model to evaluate the potential effect of wall heat transfer on soot emissions in a small-bore direct-injection diesel engine, J. Eng. Gas Turbines Power 124 (4) (2002) 1042–1052.
[37] S. Gkantonas, M. Sirignano, A. Giusti, A. D'Anna, E. Mastorakos, Comprehensive soot particle size distribution modelling of a model rich-quench-lean burner, Fuel 270 (2020) 117483.
[38] Z. Hong, D. Davidson, R. Hanson, An improved H_2/O_2 mechanism based on recent shock tube/laser absorption measurements, Combust. Flame 158 (4) (2011) 633–644.
[39] C. Olm, I. Zsély, R. Pálvölgyi, T. Varga, T. Nagy, H. Curran, T. Turányi, Comparison of the performance of several recent hydrogen combustion mechanisms, Combust. Flame 161 (9) (2014) 2219–2234.
[40] C.E. Rasmussen, C.K.I. Williams, Gaussian processes for machine learning, The MIT Press, 2006.
[41] P.G. Constantine, E. Dow, Q. Wang, Active subspace methods in theory and practice: applications to kriging surfaces, SIAM J. Sci. Comput. 36 (4) (2014) A1500–A1524.
[42] I. Sobol', Global sensitivity indices for nonlinear mathematical models and their monte carlo estimates, Math. Comput. Simul. 55 (1) (2001) 271–280.

Please cite this article as: S. Iavarone, S. Gkantonas and E. Mastorakos, Stochastic low-order modelling of hydrogen autoignition in a turbulent non-premixed flow, Proceedings of the Combustion Institute, https://doi.org/10.1016/j.proci.2022.07.129